Vegetation fires, absorbing aerosols and smoke plume characteristics in diverse biomass burning regions of Asia

2015 Environ. Res. Lett. 10 105003

(http://iopscience.iop.org/1748-9326/10/10/105003)

Environmental Research Letters

LETTER

Vegetation fires, absorbing aerosols and smoke plume characteristics in diverse biomass burning regions of Asia

Krishna Prasad Vadrevu[1], **Kristofer Lasko, Louis Giglio and Chris Justice**

Department of Geographical Sciences, University of Maryland College Park, College Park, MD 20740, USA
[1] Author to whom any correspondence should be addressed.

E-mail: Krisvkp@umd.edu

Keywords: vegetation fires, absorbing aerosols, smoke plume heights

OPEN ACCESS

RECEIVED
28 March 2015

REVISED
2 September 2015

ACCEPTED FOR PUBLICATION
8 September 2015

PUBLISHED
14 October 2015

Abstract

In this study, we explored the relationships between the satellite-retrieved fire counts (FC), fire radiative power (FRP) and aerosol indices using multi-satellite datasets at a daily time-step covering ten different biomass burning regions in Asia. We first assessed the variations in MODIS-retrieved aerosol optical depths (AOD's) in agriculture, forests, plantation and peat land burning regions and then used MODIS FC and FRP (hereafter FC/FRP) to explain the variations in AOD characteristics. Results suggest that tropical broadleaf forests in Laos burn more intensively than the other vegetation fires. FC/FRP-AOD correlations in different agricultural residue burning regions did not exceed 20% whereas in forest regions they reached 40%. To specifically account for absorbing aerosols, we used Ozone Monitoring Instrument-derived aerosol absorption optical depth (AAOD) and UV aerosol index (UVAI). Results suggest relatively high AAOD and UVAI values in forest fires compared with peat and agriculture fires. Further, FC/FRP could explain a maximum of 29% and 53% of AAOD variations, whereas FC/FRP could explain at most 33% and 51% of the variation in agricultural and forest biomass burning regions, respectively. Relatively, UVAI was found to be a better indicator than AOD and AAOD in both agriculture and forest biomass burning plumes. Cloud–Aerosol Lidar and Infrared Pathfinder Satellite Observations data showed vertically elevated aerosol profiles greater than 3.2–5.3 km altitude in the forest fire plumes compared to 2.2–3.9 km and less than 1 km in agriculture and peat-land fires, respectively. We infer the need to assimilate smoke plume height information for effective characterization of pollutants from different sources.

1. Introduction

Biomass burning is an important source of aerosols and greenhouse gas emissions in several regions of the world including Asia (Seiler and Crutzen 1980). The causative factors of biomass burning vary by region. For example, in northeast India, Eastern Ghats, northeast Myanmar, Laos and Cambodia, biomass burning has been mainly attributed to slash and burn agriculture (Toky and Ramakrishnan 1983, Prasad *et al* 2002, 2008, Palm *et al* 2013). In northwestern Thailand, the Mekong Delta in southern Vietnam, and the Punjab region of India, most of the biomass burning is attributed to agricultural residues. Farmers burn crop residues after harvest to control pests and weeds, improve soil fertility through ash and to facilitate planting of new crops (Gadde *et al* 2009, Taylor 2010, Vadrevu *et al* 2011, Kharol *et al* 2012, Sahu and Sheel 2014). In contrast, forests in the peat land burning for oil palm plantations is most common in Indonesia, Malaysia and Papau New Guinea (Carlson *et al* 2013). Also, vegetation and peatland fires in Southeast Asia have been attributed to a combination of El Nino-induced droughts and anthropogenic land-use changes (Langner *et al* 2007, Gaveau *et al* 2014). Several studies have shown that aerosols and pollutants from biomass burning can be transported long distances and persist for weeks to months, impacting not only air quality but also biogeochemical cycles, atmospheric chemistry, weather, and climate (Radojevic 2003, Cristofanelli *et al* 2014, Reddington *et al* 2014). In addition, biomass burning pollutants can have significant health impacts with increased respiratory ailments, eye irrigation, medication use and exacerbated asthma (Laumbach and Kipen 2012). It is therefore important to characterize the emissions from biomass burning sources more accurately.

One of the important indicators of aerosol amounts in the atmospheric column is aerosol optical depth (AOD), which is a measure of atmospheric extinction through a vertical column of atmosphere (Carmichael *et al* 2009). The aerosol components contributing to AOD include soot, sulfates, organics, dust, etc., and include both natural and anthropogenic sources (Barnaba and Gobbi 2004). A number of ground-based measurement stations of the AErosol RObotic NETwork (AERONET) exist in the world (Holben *et al* 1998). The AERONET consists of CIMEL sun/sky radiometers capable of retrieving aerosol optical products at discrete wavelengths ranging from 440nm (visible) to 1020 nm (near IR) (Eck *et al* 1999, Schuster *et al* 2006). The measurements from AERONET includes AOD, precipitable water, fine and coarse mode AOD including fine mode fraction, sky and surface radiance for bi-directional reflectance distribution function Due to the large temporal and spatial variability in aerosol composition and abundance, satellite retrievals of AOD became more useful for characterizing aerosols in diverse regions of the world (Myhre 2009). For example, MODIS AOD is retrieved using multiple channels onboard the Terra and Aqua satellites beginning in 2000 and 2002, with separate algorithms for oceans (Tanré *et al* 1997) and land (Kaufman *et al* 1997). The AOD's are derived by the inversion of the MODIS-observed reflectance using pre-computed radiative transfer look-up tables based on aerosol models (Remer *et al* 2002).

Satellite observations such as AOD can be a powerful tool for monitoring of atmospheric pollution if they can be related to the underlying emission sources, especially in real-time. Specific to biomass burning emissions, active fire detection and radiative power products are being used in emissions estimation in real-time such as through the Global Fire Assimilation System. The system is continuously refined to account for fire-emission amounts (Kaiser *et al* 2012). To make such operational systems robust, there is a need to evaluate and refine fire–aerosol relationships in multiple regions. Specific to Asia, most of the biomass burning aerosols are often mixed from fossil fuel combustion and dust emissions (Kaskaoutis *et al* 2009, Bucci *et al* 2014, Mishra *et al* 2014). In such a context, an important question to address is 'how much of the AOD increase is due to biomass burning and how well do satellite fire retrievals explain AOD variation?'

In this study, we characterize fire–aerosol relationships in Asia. We first assessed the variation in MODIS-retrieved AOD's in diverse biomass burning regions pertaining to agriculture, forests and plantation burning. In addition, we addressed the following questions: How well do satellite-derived fire products (fire counts (FC) and fire radiative power (FRP) (hereafter FC/FRP) correlate with different aerosol indices such as AOD, UV aerosol index (UVAI) and aerosol absorption optical depth (AAOD)? Is FRP a better indicator than FC in relating to AOD, AAOD and UVAI? What are the typical smoke plume heights in the biomass burning regions of Asia? How do smoke plume heights influence fire-AOD, AAOD, UVAI relationships? How do the correlations vary over different burning regions (i.e. agriculture versus forest versus peatland) during the peak biomass burning months? We addressed these questions using MODIS, Ozone Monitoring Instrument (OMI) and Cloud–Aerosol Lidar and Infrared Pathfinder Satellite Observation (CALIPSO) datasets.

2. Datasets and methods

We selected ten different biomass-burning windows in Asia to characterize fire–aerosol relationships (figure 1). Each window was comprised of 3×3 one-degree resolution cells (each cell with 111.3 sq.km). The dominant vegetation type burned in each window and the peak months of biomass burning are given in table 1 and figure 1. Punjab located in the northwestern region of India is dominated by rice–wheat crop rotations where agricultural residue burning is prevalent (Vadrevu *et al* 2011, 2013). Eastern Ghats are a range of discontinuous mountains situated on the east coast of India. They run from West Bengal state in the north, through Odisha and Andhra Pradesh to Tamil Nadu in the south passing some parts of Karnataka State. Biomass burning in Eastern Ghats is mostly due to slash and burn. Northeast India comprises of seven-different states in India which includes Assam, Arunachal Pradesh, Manipur, Meghalaya, Mizoram, Tripura and Nagaland. Slash and burn agriculture is most common in northeast India. The other regions include north-western Thailand with dominant rice–maize crop burning, Laos and Eastern Myanmar with tropical broadleaf forest burning, southern Vietnam (Mekong delta) with rice residue burning and Indonesia with forest/peat land fires.

We used the MERIS Globcover land cover dataset (version 2.3) for inferring the land cover types. The data set contains 22 separate land cover classes created from cloud-free mosaics of MERIS surface reflectance data and vegetation indices at a 300 m spatial resolution (Bicheron *et al* 2008). For characterizing the fire activity and FRP, the dominant land cover category was inferred to each biomass burning window based on a majority filter and the dominant vegetation type burnt based on the literature.

For characterizing fires and FRP, we used daily active fire detections from a combination of the MODIS instruments onboard the Aqua and Terra satellites. The two MODIS sun-synchronous, polar-orbiting satellites pass over the Equator at approximately 10:30 a.m./p.m. (Terra) and 1:30 p.m./a.m. (Aqua) with a revisit time of 1 to 2 days. The MODIS Advanced Processing System processes the resulting data using the enhanced contextual fire detection algorithm (Giglio *et al* 2003) combined into the Collection 5 Active Fire product. For this study, we analyzed the daily FC and FRP data for the peak biomass burning periods from 2005 to 2012 and data with more than 95% confidence level (Giglio 2009). Corresponding to the similar time-period, we used daily MODIS AOD products (MOD08_D3.005 and MYD08_D3.005) at 550 nm. To assess the statistical nature of AOD data

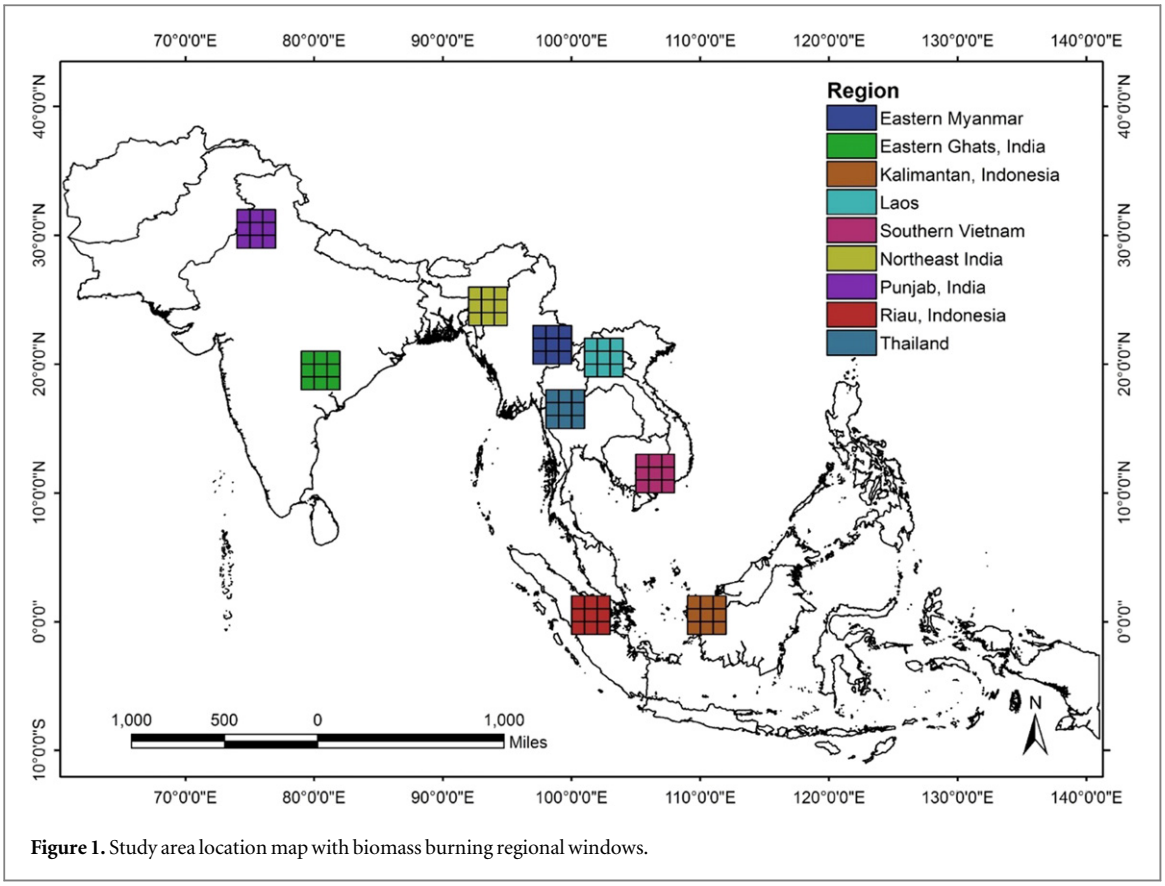

Figure 1. Study area location map with biomass burning regional windows.

Table 1. Biomass burning regions with peak biomass burning months and the type of biomass burnt.

Site	Peak biomass burning months	Dominant vegetation burnt
Thailand	February–April	Rice–maize crop residues
Southern Vietnam	February–April	Rice residues
Punjab, India-summer	March–May	Wheat residues
Punjab, India-winter	October–December	Rice residues
Riau, Indonesia	July–September	Forest/peat land fire mix
Kalimantan, Indonesia	July–September	Peat land fire mix
Eastern Ghats, India	February-April	Tropical mixed deciduous forest
Northeast India	March–May	Tropical evergreen forest
Eastern Myanmar	February–April	Broad leaf deciduous forest
Laos	February–April	Broadleaf forest

during the peak biomass burning months in different regions of Asia, we performed a frequency analysis. The MODIS AOD data were fitted to a Gaussian distribution to infer location and scale parameters as

$$y = y_0 + \frac{A}{\sigma\sqrt{\pi/2}} e^{-2\frac{(x-x_c)^2}{\sigma^2}},$$

where A is the amplitude, x_c is the center of the peak amplitude, and σ (sigma) is the width at half peak amplitude.

The AAOD is a columnar measure of concentration of near-UV absorbing aerosol particles such as smoke and mineral dust and is retrieved from the OMI (Bucsela *et al* 2008). We used the AAOD daily product at 500 nm (OMAERUVd.003). In addition, we also used UV aerosol index (UVAI) that detects the presence of UV-absorbing aerosols such as dust and soot. UVAI is based on a spectral contrast method in a UV region where the ozone absorption is very small. It is the difference between the observations and model calculations of absorbing and non-absorbing spectral radiance ratios. For OMI, AI is defined as

$$\mathrm{AI} = 100\Big[\log_{10}\big(I_{360}/I_{331}\big)_{\mathrm{measured}} - \log_{10}\big(I_{360}/I_{331}\big)_{\mathrm{calculated}}\Big].$$

Positive values of AI generally represent absorbing aerosols (dust and smoke) while small or negative values represent non-absorbing aerosols (sulfate, sea-salt) and clouds (Torres *et al* 2007). We specifically used the daily product (OMTO3d.003) to infer UVAI variations. Both the AAOD and UVAI variations were assessed using histograms with mean and standard deviation. To address fire-AOD, AAOD and UVAI

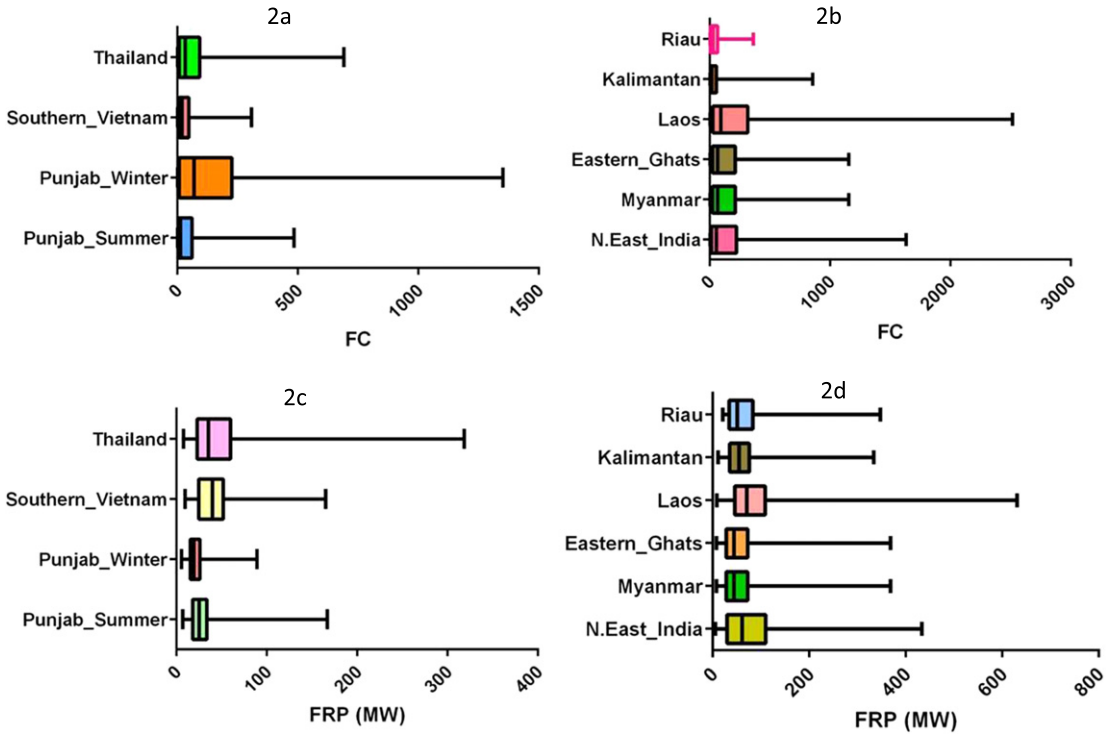

Figure 2. (a)–(d) Variations in fire counts (FC) (a), (b) and FRP (c), (d) in different biomass burning regions. The box and whisker plots show minimum to maximum values in FC and FRP, respectively. Figures 2(a) and (b) refer to agricultural burning regions; whereas except for Riau and Kalimantan (forest/peat land mix fires), the other regions in (b) and (d) refer to forest biomass burning regions. Refer to table 1 for the peak biomass burning months and dominant vegetation type burned.

relationships, we used linear regression with 95% confidence interval bands.

To attribute the differences in fire-AOD relationships, we used the CALIPSO data. The vertical distribution of aerosol information is inferred through the analysis of backscatter measurements provided by the Cloud–Aerosol Lidar with Orthogonal Polarization (CALIOP) instrument onboard the CALIPSO satellite of the NASA A-Train (Winker 2007, Hunt *et al* 2009). The CALIPSO product is highly useful in discriminating aerosol layers from clouds (Liu *et al* 2009), categorizing aerosol layers as one of six subtypes (dust, marine, smoke, polluted dust, polluted continental, and clean continental; Omar *et al* 2009), and for estimating the optical depth of each layer detected (Vaughan *et al* 2004). In this study, we specifically used the CAL_LID_L1-ValStage1-V3-30 datasets; averaged three to four mostly night-time passes during the peak biomass burning periods for each window as the CALIPSO provides information every 16 days (Winker 2007). We used the total attenuated backscatter coefficient at 532 nm and smoke altitude information for characterizing aerosol concentrations during the biomass burning months for different regional windows (figure 1).

3. Results

3.1. FC variations (2005–2012)

The sum of FC for the peak biomass burning months in a typical 3 × 3 one degree resolution window for different biomass burning regions are shown in box and whisker plots with the bottom and top of the box representing first and third quartiles, the band inside the box with median values, and the tails representing the minimum to the maximum FC (figures 2(a) and (b)). In agricultural biomass burning regions, highest FC were found during the Punjab winter season (1350FC) followed by Thailand, Punjab summer and Southern Vietnam. The median FC values were higher for Punjab winter data compared to the others (figure 2(a)). Of the different regions, Laos with the broadleaf forest burning had the highest FC (2596) and lowest FC in Riau, Indonesia including the median values (figure 2(b)).

3.2. FRP variations

Amongst the agricultural biomass burning regions, maximum FRP was found for Thailand (318.3 MW) followed by Punjab during summer (figure 2(c)). Among the forest, plantation and peat land fires, Laos had the highest FRP (630.7 MW) and lowest for Kalimantan peat land fires (338.8 MW) (figure 2(d)). These results clearly suggest more intense biomass burning from tropical broadleaf forests (Laos) than from agriculture and peat land fires.

3.3. AOD variations

Biomass burning activities are expected to increase AOD's compared to the background (Badarinath *et al* 2007, 2009, Eck *et al* 2009). Figures 3(a)–(j) summarizes the MODIS-retrieved AODs based on the fitted Gaussian model. For the normal distribution, the location and scale parameters

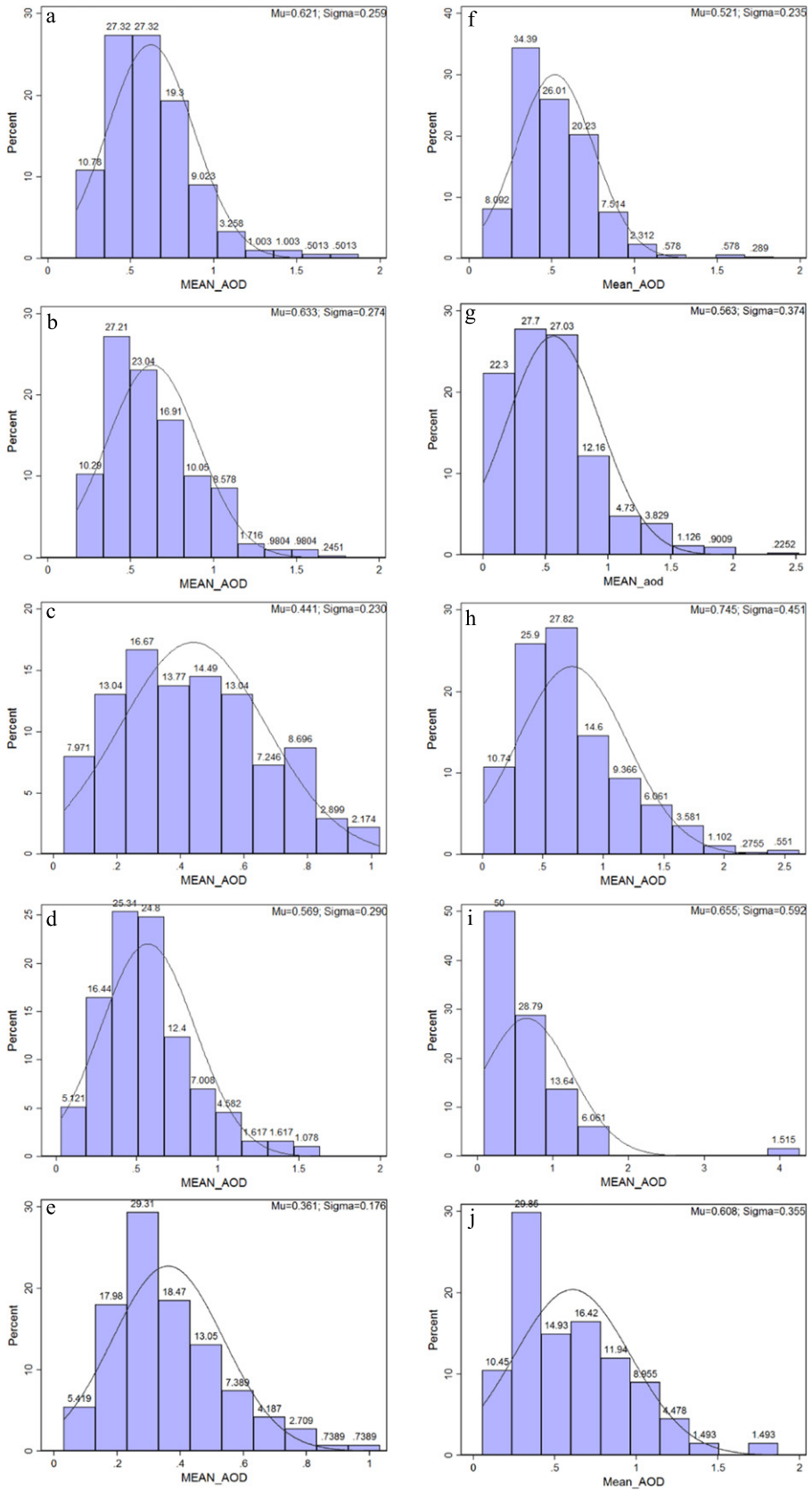

Figure 3. (a)–(i) AOD Frequency plots with normal distribution for different biomass burning windows. Mean and sigma values are also shown in the plots. (a) Punjab, summer, India; (b) Punjab, winter, India; (c) Southern Vietnam; (d) Thailand; (e) Eastern Ghats, India; (f) Northeast India; (g) Eastern Myanmar; (h) Laos; (i) Riau, Indonesia; (j) Kalimantan, Indonesia.

correspond to the mean (μ) (given as Mu in figures) and standard deviation (sigma). For example, in the entire dataset, the mean AOD was relatively high for Laos ($\mu = 0.75$) broadleaf forest burning (figure 3(h)) compared to the other vegetation types including agriculture categories 3(a)–(d). Similarly, Riau province, Indonesia with the forest/peat land mix fires (figure 3(i)) had the highest sigma values (0.592) compared to the other forest

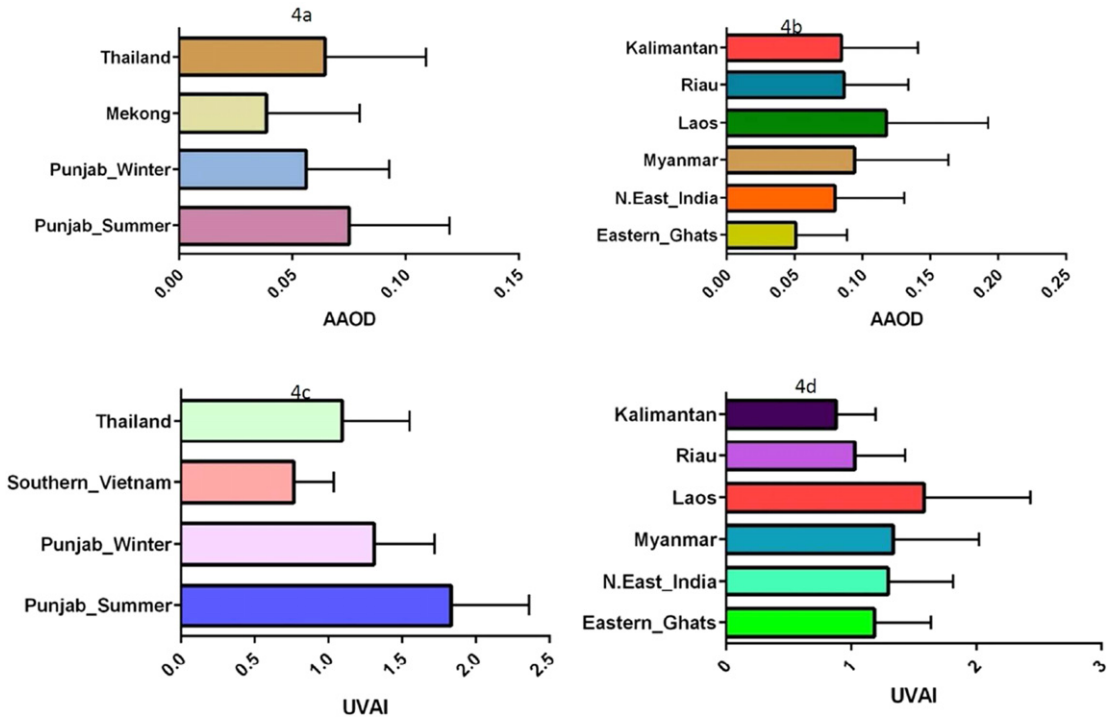

Figure 4. (a)–(d) Variations in AAOD (a), (b) and UVAI (c), (d) in different biomass burning regions. The column bar graphs show mean with standard deviation.

burning regions. Among the forest types, tropical mixed deciduous forest in Eastern Ghats (figure 3(e)) had the lowest mean AOD (0.361) and sigma (0.178). Further, among the crop residue burning regions, Punjab, India had the highest mean both in summer (figure 3(a)) as well as winter (figure 3(b)) ($\mu = 0.621$ and 0.633, respectively), whereas, southern Vietnam with rice residue burning (figure 3(c)) had the lowest mean AOD (0.441). We also note that forest/peat land mix biomass burning regions had relatively higher standard deviations indicating higher variability in AOD compared to the agricultural regions.

3.4. AAOD variations

AAOD variations for different sites are shown as histograms with mean and standard deviation (figures 4(a) and (b)). Among the agricultural biomass burning regions, Punjab during the summer season had the highest mean AAOD (0.075) and lowest in Southern Vietnam (0.038) (figure 4(a)). The standard deviation in AAOD values was similar (0.044) for Punjab, Southern Vietnam, and Thailand and lowest during the Punjab winter season (0.036) (figure 4(b)). Among the forest, plantation and peat land fires, Laos and Myanmar with forest biomass burning had the highest AAOD (0.117) and Eastern Ghats the lowest (figure 4(b)).

3.5. UVAI variations

Similar to AAOD, Punjab during the summer season showed highest mean UVAI (1.83) (figure 4(c)). Among the forested biomass burning regions, Laos had the highest mean UVAI (1.58) and the lowest for the peat-land fires in Kalimantan (0.87) (figure 4(d)).

3.6. FC-AOD and FRP-AOD correlations

FC-AOD correlations (figures A1(a)–(i) in appendix) in different agricultural regions did not exceed 20% (figures A1(a)–(d) in appendix). Highest FC-AOD correlations were found for Thailand and Punjab winter burning (both with $r^2 = 0.20$ (figures A1(d), (b)) and lowest for Punjab-summer burning ($r^2 = 0.08$) (figure A1(a)). With the exception in southern Vietnam, FRP-AOD correlations were consistently weak in different agricultural systems and less than FC-AOD relationships. FC-AOD correlations in forest, plantation and peat land fires were relatively higher than the agricultural systems with highest correlation ($r^2 = 0.34$) in Myanmar A1(g) and lowest in Riau province ($r^2 = 0.02$) (figure A1(i)). FRP-AOD correlations were relatively higher for Myanmar ($r^2 = 0.40$) (figure A3(g)) compared to the others.

3.7. FC-AAOD and FRP-AAOD Correlations

Our results indicate comparatively lower correlations between FC-AAOD and FRP-AAOD in agricultural systems than in forest systems (figures A1–A2(a)–(i), appendix). In agricultural systems, the highest FC-AAOD correlation was found for Thailand ($r^2 = 0.29$) (figure A1(d)) and lowest for southern Vietnam ($r^2 = 0.078$) (figure A1(c)). Further, FC-AAOD and FRP-AAOD correlations were almost similar in agricultural systems. Among the forest biomass burning regions, the highest FC-AAOD correlation was in Laos ($r^2 = 0.53$) (figure A1(h)) and lowest in Riau province ($r^2 = 0.18$) (figure A1(i)).

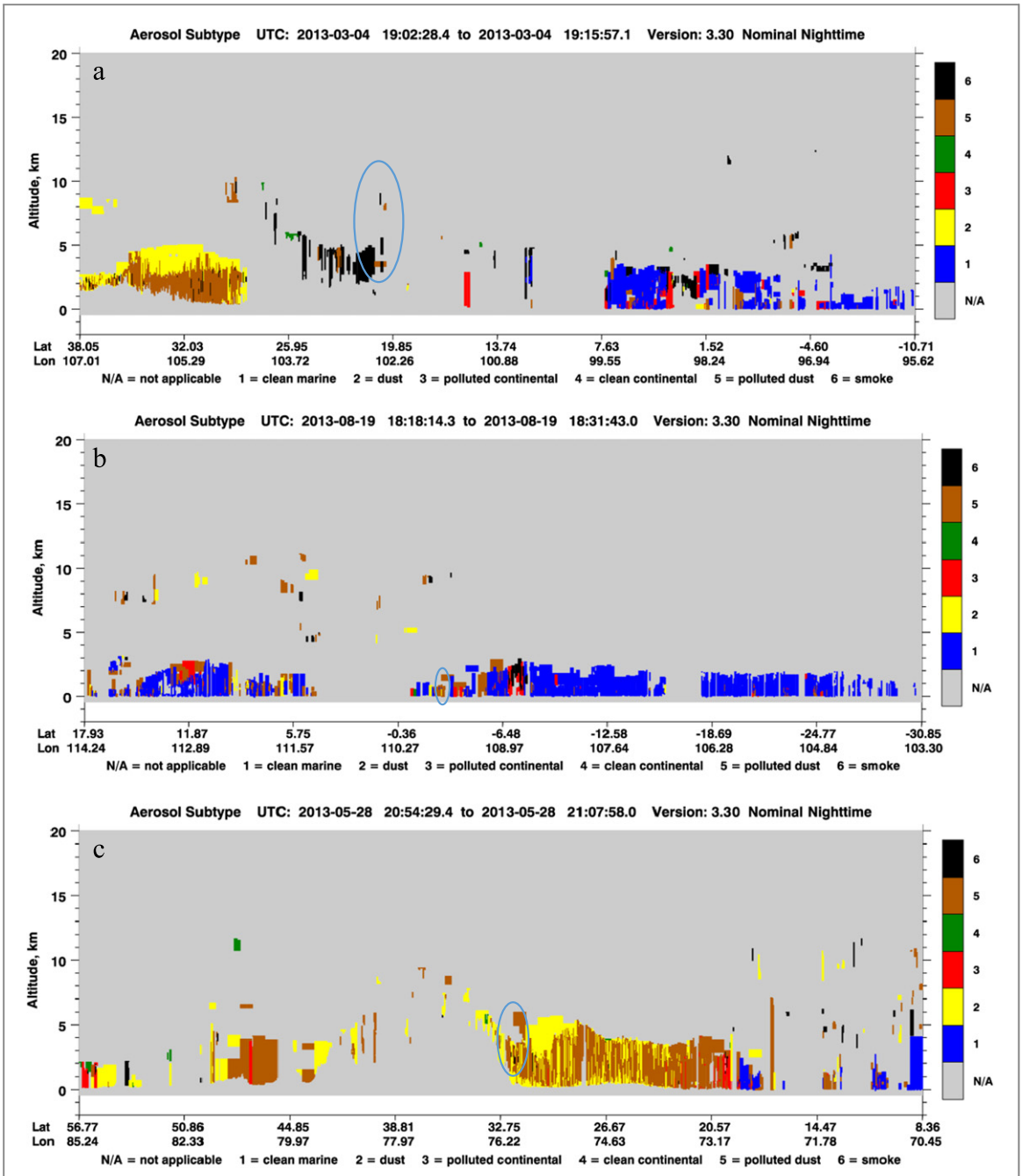

Figure 5. (a)–(c) Smoke plume characteristics in different biomass burning regions retrieved from CALIPSO data. Specific biomass burning regions are highlighted in blue elliptic circles. (a) Laos with smoke plume altitude (~5.3 km) representing broad leaf forest burning; (b) Kalimantan, Indonesia with smoke plume altitude (800 m) representing peat-land fires; (c) Punjab, India, smoke plume heights (2.3 km) during summer agricultural residue burning. Polluted dust aerosols above 5 km can also be seen in the blue elliptic circle in orange color (in contrast to smoke in black color).

3.8. FC-UVAI and FRP-UVAI correlations

These correlations in agricultural systems were much stronger than FC-AOD and FC-AAOD correlations (figures A1–A4(a)–(j), appendix). Amongst the agricultural systems, FC-UVAI correlation was highest in Thailand (0.33) (figures A2(d)) and lowest during the Punjab-summer season ($r^2 = 0.14$) (figure A2(a)). FRP-UVAI correlations were similar to FC-UVAI correlations in agricultural systems. Further, FC-UVAI correlations in forest, plantation and peat land fires were relatively higher than the agricultural systems with the highest correlation in Laos ($r^2 = 0.51$) (figure A2(h)) and lowest in Riau province ($r^2 = 0.20$) (figure A2(i)). Also, FRP-UVAI correlations were relatively stronger for forests than agriculture and peatland fires.

In summary, the correlation analysis suggested the following: (a) The FC/FRP versus AOD, AAOD and UVAI correlations were stronger for forest, plantation and peat land fires than the agricultural fires; (b) Among the aerosol indices, UVAI was more strongly correlated with FC or FRP followed by AAOD and AOD in both forest, peat land and plantation/peat land mix fires than the agricultural fires; (c) Our results indicate that that the sum of FRP was better correlated with UVAI than AOD or AAOD in forest

Table 2. Smoke plume and Polluted dust altitudes for different biomass burning regions retrieved using CALIOP data. Highest smoke plume altitudes (5.3 km) can be seen for Laos tropical broad-leaf forest biomass burning and lowest for Kalimantan, Indonesia peat land fires (800 m). Relatively higher backscatter values were noted for forest biomass burning sites compared to the agriculture and peat land fires.

Site	Smoke altitude (Km)	Polluted dust altitude (Km)	CALIPSO 532 nm total attenuated backscatter, $km^{-1}\,sr^{-1}$
Thailand	3.9	2.8	3×10^{-2}
Southern Vietnam	1.3	2.2	4×10^{-3}
Punjab, India-summer	2.3	5.2	2.5×10^{-3}
Punjab, India-winter	2.5	2.9	4.5×10^{-3}
Riau, Indonesia	3.2	3	5.0×10^{-3}
Kalimantan, Indonesia	800 m	1	4.5×10^{-3}
Eastern Ghats, India	3.2	3.6	5.0×10^{-3}
Northeast India	4.8	4.9	7.0×10^{-2}
Eastern Myanmar	4.9	2.5	5.5×10^{-3}
Laos	5.3	3.5	6.5×10^{-2}

biomass burning regions. Further, we found UVAI as better indicator than AOD or AAOD and correlating well with FRP than FC in forest, plantation and peat land fires.

3.9. CALIPSO observations

In table 2, CALIPSO-derived 532 nm backscatter values as well as smoke plume heights for different biomass burning regions and aerosol sub-types with plume heights for sample regions in figures 5(a)–(c). Vertical profiles of aerosol concentrations showed maximum concentrations over the forested regions compared to the agricultural biomass burning sites (table 2). Specific to the agricultural residue burning sites, aerosol loading is found to be highest for Thailand (3×10^{-2}/sr/km) followed by Punjab-winter season (4.5×10^{-3}/sr/km) and lowest for southern Vietnam. Aerosols reaching the highest altitude have been noted for Thailand (3.9 km) and lowest for southern Vietnam (2.2 km). Eastern Ghats, India as well as Kalimantan and Riau province, Indonesia had relatively low smoke plume altitudes than other forest biomass burning sites.

4. Discussion

The above results suggest that a broad distinction can be made between the aerosol properties and smoke plume heights of agricultural versus forest biomass burning regions. Most of the forest biomass burning regions had relatively higher median FC and FRP. Results clearly suggest that tropical broadleaf forests in Laos burn more intensively (higher FRP) than the other forest types, peat lands as well as agricultural regions. Higher FRP from forests may be attributed to relatively higher biomass per unit area compared to agriculture and peatlands. However, more verification is needed to delineate FRP variations in the field. As in several other studies (Ramanathan *et al* 2001, Eck *et al* 2009, Lin *et al* 2014), we noted increase in AOD during the biomass burning months. The mean AOD during the peak biomass burning periods in the Laos exceeded 0.75. Similarly in the agricultural biomass burning regions mean AOD was greater than 0.60 in Punjab summer as well as during winter residue burning. Although AOD is a good indicator of overall air pollution, increase in AOD may be attributed to a variety of other such as dust aerosols (Kim *et al* 2007, Vadrevu *et al* 2011). Further, MODIS AOD can only be retrieved under clear-sky conditions and under partially cloudy skies the probability of subpixel cloud contamination can be larger (Xia *et al* 2013).

The main aerosol released from biomass burning that causes large variations in the atmospheric chemistry and radiation budget is black carbon, which is the optically absorbing part of the carbonaceous aerosols (Saha and Despiau 2009). In particular, OMI AAOD is an indicator of absorbing carbonaceous aerosols resulting from biomass burning activity (Torres *et al* 2010). The AAOD values for agricultural fires varied from 0.03–0.07 to 0.08–0.11 for the forest/plantation and peat land mixed fires. These values clearly suggest biomass burning from forest fires release much more absorbing aerosols than the agricultural fires. The AAOD values reported for forest biomass burning in our study were comparatively lower than the AAOD values reported for fire plumes in South America and Central Africa. For example, Torres *et al* (2010) during the five-year analysis period reported the peak monthly AAOD values in the range of 0.08–0.15 during September in the South America. They also reported peak monthly AAOD values between 0.08 and 0.12 during August in Central Africa. Although we observed relatively higher FC-AAOD and FRP-AAOD correlations for the forest/plantation peat land mix fires than the agricultural fires, the correlation within the sites between FC and FRP with AAOD were not much different. Further the higher correlations observed between FC/FRP-AAOD compared to FC/FRP-AOD suggests AAOD as a better indicator of absorbing aerosols for forest and plantation peat land mix fires.

Specific to the OMI-UVAI, earlier, Torres *et al* (1998, 2007, 2010), Hsu *et al* (1999), and Ginoux and Torres (2003) noted an important sensitivity of OMI to UV absorbing aerosols as a function of smoke plume heights. Also, Torres *et al* (1998, 2012) showed that the magnitude of the positive AI depends on the AAOD and height of the aerosol layers. They also showed that AI signal is meaningful above 0.5 and AI signal is amplified when the absorbing layer lies above the clouds. In essence,

OMI AI can be retrieved when mixed with clouds but its sensitivity increases significantly when the absorbing aerosol layers are located above clouds (Xia *et al* 2013). In addition, Badarinath *et al* (2009) and Guan *et al* (2010) have shown increasing AI greater than 1.5 in biomass burning plumes. Similar to these studies, we found UVAI to be a good indicator of enhanced aerosols from biomass burning, as the values were significantly high varying from 1.0 to 1.8 in agricultural biomass burning plumes and 0.8–1.58 UVAI in forest and plantation/peat land mix fires. Consistently strong correlations (0.40–0.51) between FC-UVAI and (0.40–0.52) between FC-FRP were observed among the forest fires in Eastern Ghats, Northeast India, Myanmar and Laos compared to FC/FRP-AOD and may be attributed to release of smoke plumes above clouds that could be effectively detected by OMI data (Torres *et al* 2010) compared to MODIS. In contrast, the relatively weak FC/FRP-UVAI correlations in peat and agricultural biomass burning regions may be attributed to low smoke plumes heights. To test the relative differences in smoke plume heights in agricultural and forest and plantation peat land mix fires, we evaluated the CALIPSO data.

Large amounts of smoke aerosol can be injected into the atmosphere as a result of biomass burning. Literature review suggest that, unlike clouds, thin smoke plumes have a weak 532 nm total attenuated backscatter signal and dense plumes may have a 532 nm backscatter signal similar to clouds (Winker 2007, Omar *et al* 2009). In our case, the overall CALIPSO backscatter values at 532 nm were considerably higher for the forest biomass burning sites than the agricultural sites (figures 5(a)–(c)).

For example, Mishra *et al* (2014) reported 2.32–3.58 $\times$ 10^{-3} sr km^{-1} for the Indo-Ganges region close to our reported values of 2.5 $\times$ 10^{-3} sr km^{-1} for Punjab during the summer biomass burning region. In the Punjab winter biomass burning season, we observed higher backscatter values compared to the summer. This may be due to relatively low dust signal during winter compared to the summer. High smoke plume altitudes for the dust aerosols can be seen in figure 5(c) for the Punjab summer season. We also note comparable smoke plume heights for Punjab during both summer and winter. Overall, the smoke plume heights for agricultural regions were considerably lower than the forest biomass burning sites. Further, in Kalimantan, Indonesia lowest smoke plume heights were observed with less than 1 km. Similar results were reported by Tosca *et al* in the range of 709 $\pm$ 14 m on Borneo and 749 $\pm$ 24 m on Sumatra and attribute it to low fire intensities from smoldering peat-land fires compared to the large boreal crown fire plumes of Alaska, or the higher-intensity grass fires of Australia (Kahn *et al* 2008, Mims *et al* 2010). Further, in our study, UVAI values varied from 0.87 to 1.87 in the Kalimantan region compared to 1–02–4.2 UVAI values observed for other forest biomass burning regions. These differences clearly suggest increased pyro-convection of aerosols over the forest biomass burning regions than the agriculture as well as peat-land fires thus impacting FC/FRP-AOD, AAOD and UVAI correlations. As UVAI is sensitive to aerosols that aloft above the clouds, it can be used effectively in conjunction with AAOD and FC/FRP to relate to biomass burning aerosols in forest biomass burning regions. We also found smoke altitudes as key for relating FC or FRP with AOD, AAOD, UVAI in different biomass burning regions of Asia. More specifically, relating FC/FRP to UVAI may be more justified than using AOD alone as the UVAI is a robust indicator of absorbing aerosols mainly from biomass burning compared to AOD which is mixed signal from several other aerosols apart from biomass burning. For resolving inter-annual differences in FC/FRP and aerosol indices, more in-depth studies are needed. Variations in FC/FRP and correlations with the other atmospheric satellite data products suggested distinct patterns among different biomass burning regions and the significance of UV based aerosol index. We also infer the need to assimilate smoke plume height data such as from CALIPSO for operational monitoring of pollutants from different sources including biomass burning to reduce uncertainties.

5. Conclusions

Fire–aerosol characteristics were studied using daily multi-satellite data during the peak biomass burning periods in different regions of Asia. MODIS FC as well as FRP products were useful in characterizing fire events and intensities. We found relatively lower FRP's over the agricultural and peat land fire regions compared to forest biomass burning regions. In the study, we also tested the relationship between FC/FRP and various aerosol products such as AOD, AAOD and UVAI in biomass burning regions. Of the different products, we found UVAI as a better indicator of biomass burning pollution and strongly relating to FC/FRP in forest biomass burning than the agricultural biomass burning regions. We used the CALIPSO data to infer poor/strong correlations of FC/FRP in agriculture and forest biomass burning regions. Results suggested significantly higher CALIPSO backscatter as well as smoke plume heights for forest biomass burning regions than agriculture and peat-land fires. The results highlight FC/FRP-AOD, AAOD and UVAI relationships in different biomass burning regions in addition to smoke plume characteristics useful to address biomass burning pollution on atmosphere and climate.

Acknowledgments

We thank product developers of MODIS, MERIS, OMI and CALIPSO for free sharing of products. This research was supported by NASA grant NNX10AU77G.

Appendix

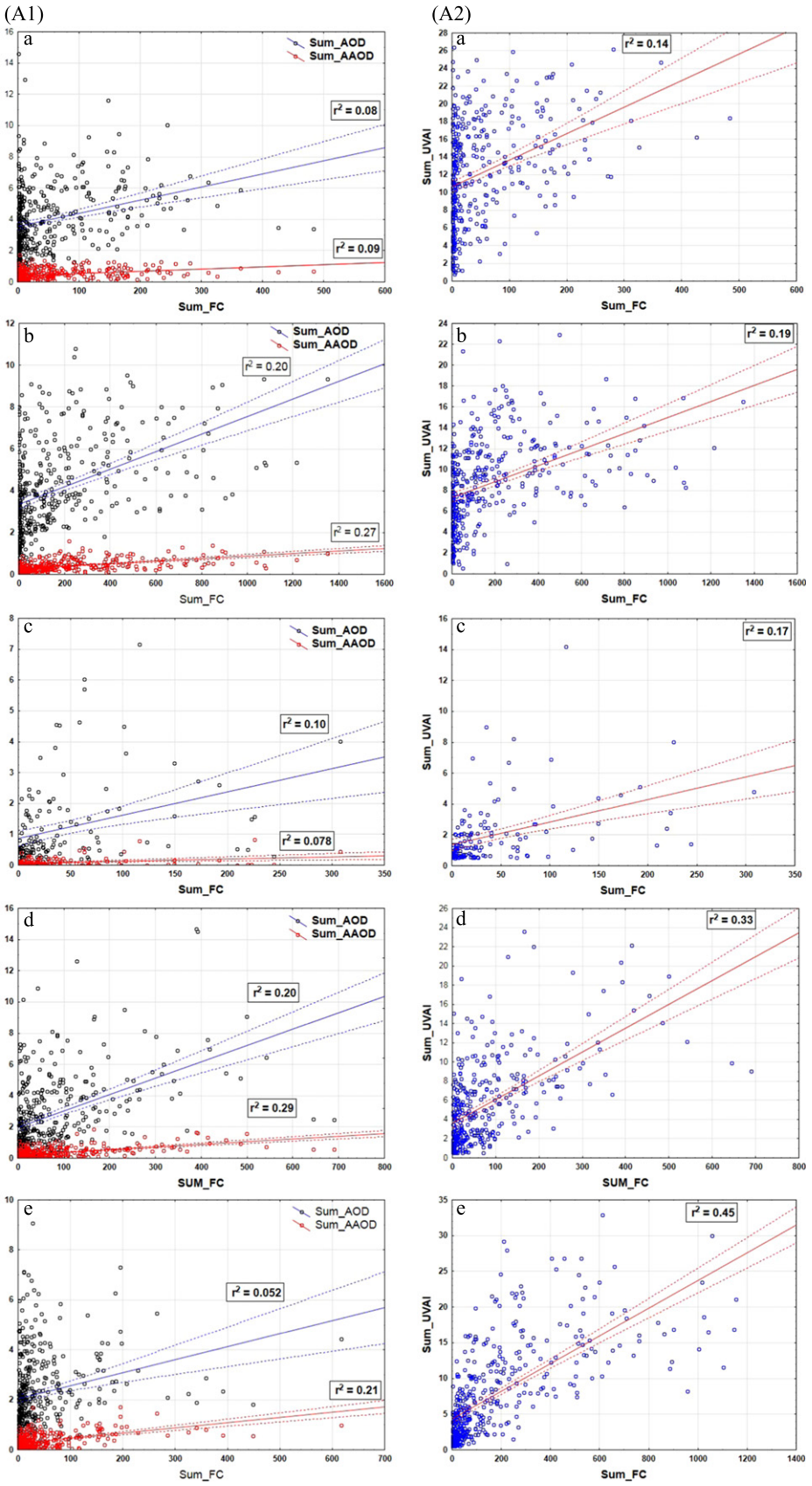

Figure A1–A2. (a)–(j) Scatterplots between sum of FC-AOD, Sum of FC-AAOD A1(a)–(j) and sum of FC-UVAI relationships A2(a)–(j). R-square linear fit and regression bands at 95% confidence interval are also shown. A1–A2(a) Punjab, summer, India; A1–A2(b) Punjab, winter, India; A1–A2(c) Southern Vietnam; A1–A2(d) Thailand; A1–A2(e) Eastern Ghats, India; A1–A2(f) Northeast India; A1–A2(g) Eastern Myanmar; A1–A2(h) Laos; A1–A2(i) Riau, Indonesia; A1–A2(a), (j) Kalimantan, Indonesia.

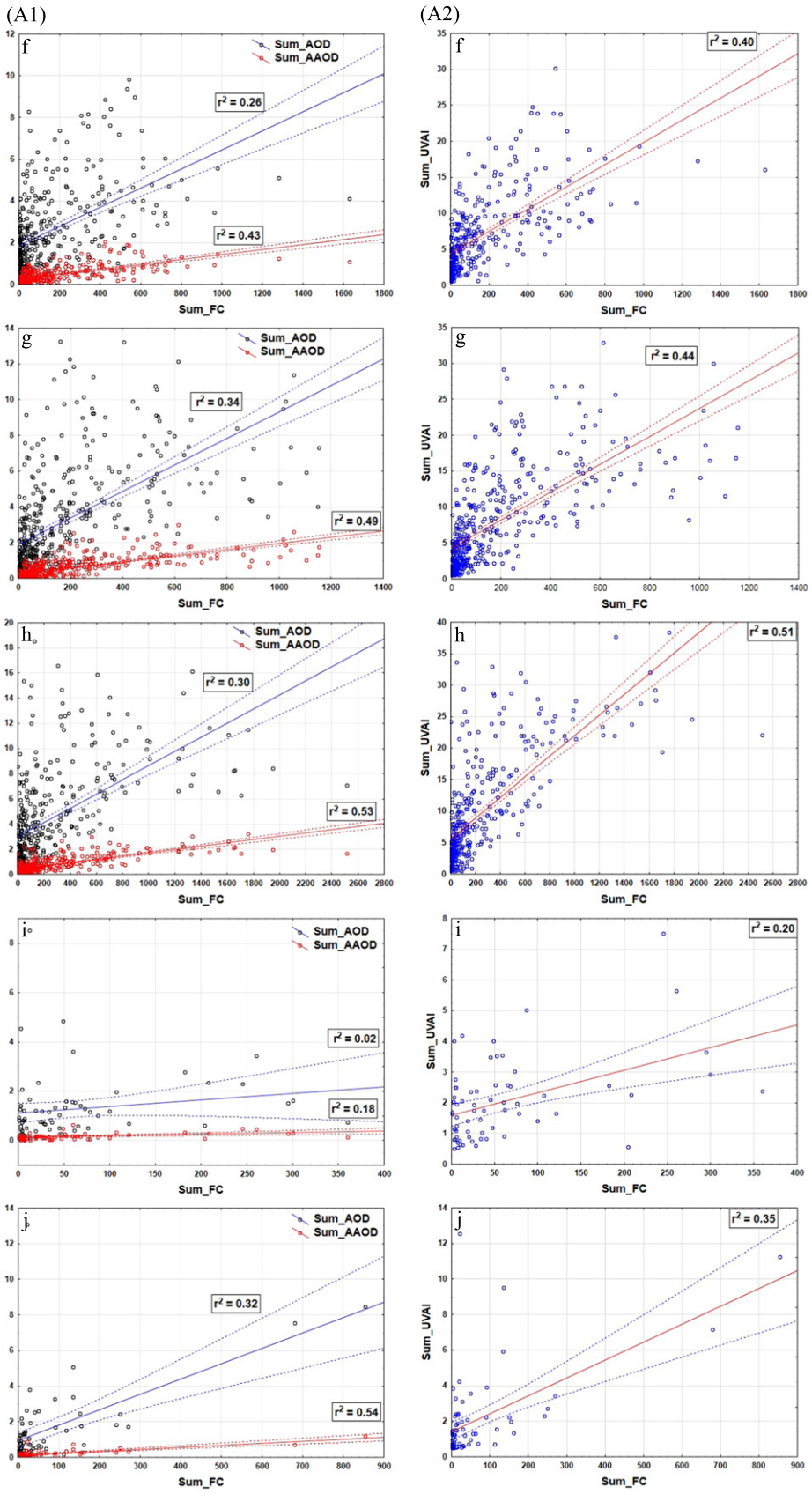

Figure A1–A2. (Continued.)

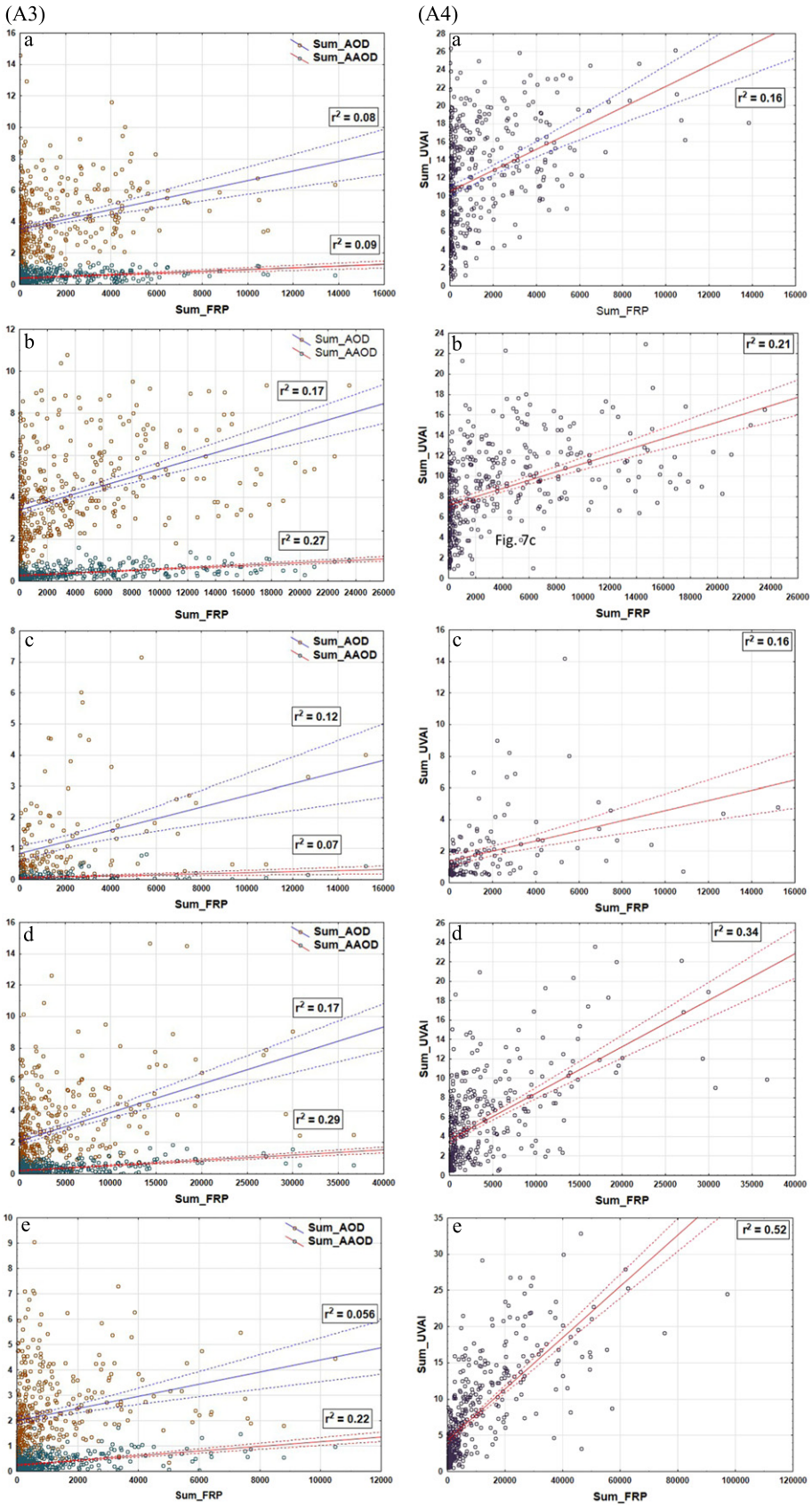

Figure A3–A4. (a)–(j) Scatterplots between sum of FRP-AOD, sum of FRP-AAOD A3(a)–(j) and sum of FRP-UVAI relationships A4(a)–(j). R-square linear fit and regression bands at 95% confidence interval are also shown. A3–A4(a) Punjab, summer, India; A3–A4(b) Punjab, winter, India; A3–A4(c) Southern Vietnam; A3–A4(d) Thailand; A3–A4(e) Eastern Ghats, India; A3–A4(f) Northeast India; A3–A4(g) Eastern Myanmar; A3–A4(h).Laos; A3–A4(i) Riau, Indonesia; A3–A4(j) Kalimantan, Indonesia.

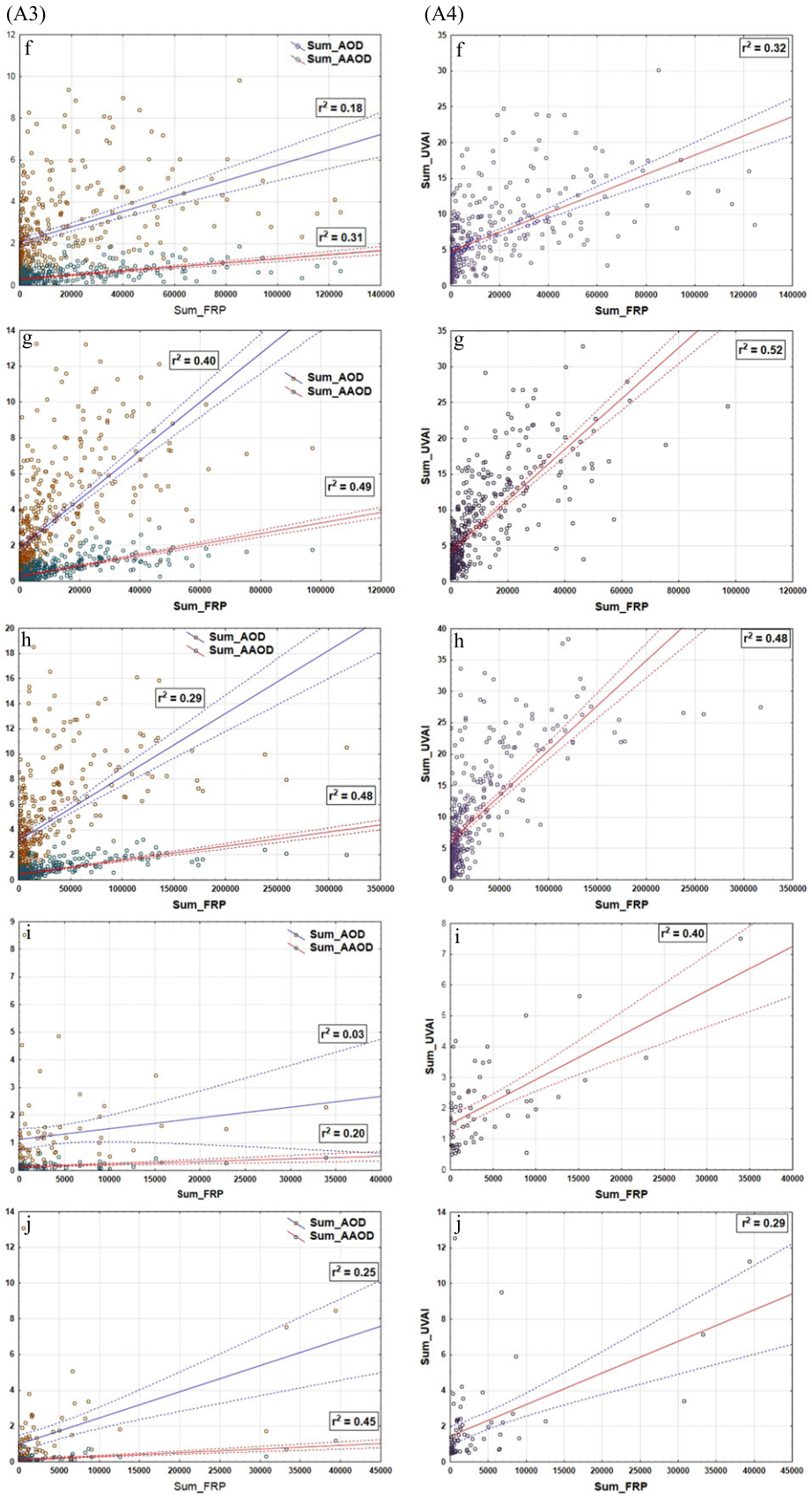

Figure A3–A4. (Continued.)

References

Badarinath K V S *et al* 2007 Multiyear ground-based and satellite observations of aerosol properties over a tropical urban area in India *Atmos. Sci. Lett.* **8** 7–13

Badarinath K V S *et al* 2009 Analysis of aerosol and carbon monoxide characteristics over Arabian Sea during crop residue burning period in the Indo-Gangetic Plains using multi-satellite remote sensing datasets *J. Atmos. Sol.—Terr. Phys.* **71** 1267–76

Barnaba F and Gobbi G P 2004 Aerosol seasonal variability over the Mediterranean region and relative impact of maritime, continental and Saharan dust particles over the basin from MODIS data in the year 2001 *Atmos. Chem. Phys.* **4** 2367–91

Bicheron P *et al* 2008 Geo-location assessment of MERIS GlobCover ortho-rectified products *Proc. 2nd MERIS-AATSR Workshop* (*Frascati, Italy, 22–26 September 2008*) SP-666

Bucci S, Cagnazzo C, Cairo F, Di Liberto L and Fierli F 2014 Aerosol variability and atmospheric transport in the Himalayan region from CALIOP 2007–2010 observations *Atmos. Chem. Phys.* **14** 4369–81

Bucsela E J *et al* 2008 Comparison of tropospheric NO_2 from *in situ* aircraft measurements with near real-time and standard product data from OMI *J. Geophys. Res.* **113** 2156–202

Carlson K M, Curran L M, Asner G P, Pittman A M, Trigg S N and Adeney J M 2013 Carbon emissions from forest conversion by Kalimantan oil palm plantations *Nat. Clim. Change* **3** 283–7

Carmichael G R *et al* 2009 Asian aerosols: current and year 2030 distributions and implications to human health and regional climate change *Environ. Sci. Technol.* **43** 5811–7

Cristofanelli P *et al* 2014 Transport of short-lived climate forcers/pollutants (SLCF/P) to the Himalayas during the South Asian summer monsoon onset *Environ. Res. Lett.* **9** 084005

Eck T F *et al* 1999 Wavelength dependence of the optical depth of biomass burning, urban, and desert dust aerosols *J. Geophys. Res.* **104** 31333–49

Eck T F *et al* 2009 Optical properties of boreal region biomass burning aerosols in central Alaska and seasonal variation of aerosol optical depth at an Arctic coastal site *J. Geophys. Res.* **114** D11201

Gadde B, Menke C and Wassmann R 2009 Rice straw as a renewable energy source in India, Thailand, and the Philippines: overall potential and limitations for energy contribution and greenhouse gas mitigation *Biomass and Bioenergy* **33** 1532–46

Gaveau D L *et al* 2014 Major atmospheric emissions from peat fires in Southeast Asia during non-drought years: evidence from the 2013 Sumatran fires *Sci. Rep.* **4** 6112

Giglio L *et al* 2003 An enhanced contextual fire detection algorithm for MODIS *Remote Sens. Environ.* **87** 273–82

Giglio L *et al* 2009 An active-fire based burned area mapping algorithm for the MODIS sensor *Remote Sens. Environ.* **113** 408–20

Ginoux P and Torres O 2003 Empirical TOMS index for dust aerosol: applications to model validation and source characterization *J. Geophys. Res.* **108** 4534

Guan H *et al* 2010 A multi-decadal history of biomass burning plume heights identified using aerosol index measurements *Atmos. Chem. Phys.* **10** 6461–9

Holben BN *et al* 1998 AERONET—A federated instrument network and data archive for aerosol characterization *Remote Sens. Environ.* **66** 1–16

Hsu NC *et al* 1999 Comparisons of the TOMS aerosol index with Sun-photometer aerosol optical thickness: results and applications *J. Geophys. Res.* **104** 6269–79

Hunt WH *et al* 2009 CALIPSO lidar description and performance assessment *J. Atmos. Ocean. Technol.* **26** 1214–28

Kahn R A *et al* 2008 Wildfire smoke injection heights: two perspectives from space *Geophys. Res. Lett.* **35** L04809

Kaiser JW *et al* 2012 Biomass burning emissions estimated with a global fire assimilation system based on observed fire radiative power *Biogeosci.* **9** 527–54

Kaskaoutis DG *et al* 2009 Variations in the aerosol optical properties and types over the tropical urban site of Hyderabad, India *J. Geophys. Res.* **114** D22204

Kaufman YJ *et al* 1997 Operational remote sensing of tropospheric aerosol over land from EOS moderate resolution imaging spectroradiometer *J. Geophys. Res.* **102** 17051–67

Kharol SK *et al* 2012 Black carbon aerosol variations over Patiala city, Punjab, India—a study during agriculture crop residue burning period using ground measurements and satellite data *J. Atmos. Sol.—Terr. Phys.* **84** 45–51

Kim S-W *et al* 2007 Seasonal and monthly variations of columnar aerosol optical properties over east Asia determined from multi-year MODIS, LIDAR, and AERONET sun/sky radiometer measurements *Atmos. Environ.* **41** 1634–51

Langner A, Miettinen J and Siegert F 2007 Land cover change 2002–2005 in Borneo and the role of fire derived from MODIS imagery *Glob.Change Biol.* **13** 2329–40

Laumbach R J and Kipen H M 2012 Respiratory health effects of air pollution: update on biomass smoke and traffic pollution *J. Allergy Clin. Immunology* **129** 3–11

Lin NH *et al* 2014 Interactions between biomass-burning aerosols and clouds over Southeast Asia: current status, challenges, and perspectives *Environ. Pollut.* **195** 292–307

Liu Z *et al* 2009 The CALIPSO lidar cloud and aerosol discrimination: Version 2 algorithm and initial assessment of performance *J. Atmos. Ocean. Technol.* **26** 1198–213

Mims SR *et al* 2010 MISR stereo heights of grassland fire smoke plumes in Australia IEEE Transactions on *Geosci. Remote Sens.* **48** 25–5

Mishra AT, Shibata T and Srivastava A 2014 Synergistic approach for the aerosol monitoring and identification of types over Indo-Gangetic Basin in Pre-Monsoon Season *Aerosol Air Qual. Res.* **14** 767–82

Myhre G 2009 Consistency between satellite-derived and modeled estimates of the direct aerosol effect *Science* **325** 187–90

Omar AH *et al* 2009 The CALIPSO automated aerosol classification and lidar ratio selection algorithm *J. Atmos. Ocean. Technol.* **26** 1994–2014

Palm CA *et al* 2013 *Slash-and-Burn Agriculture: The Search for Alternatives* (New York: Columbia University Press)

Prasad VK, Badarinath KVS and Eaturu A 2008 Biophysical and anthropogenic controls of forest fires in the Deccan Plateau, India *J. Environ. Manage.* **86** 1–13

Prasad VK *et al* 2002 Biomass burning and related trace gas emissions from tropical dry deciduous forests of India: a study using DMSP-OLS data and ground-based measurements *Int. J. Remote Sens.* **23** 2837–51

Radojevic M 2003 Chemistry of forest fires and regional haze with emphasis on Southeast Asia *Pure Appl. Geophys.* **160** 157–87

Ramanathan VC *et al* 2001 Aerosols, climate, and the hydrological cycle *Science* **294** 2119–24

Reddington C L *et al* 2014 Contribution of vegetation and peat fires to particulate air pollution in Southeast Asia *Environ. Res. Lett.* **9** 094006

Remer L A *et al* 2002 Validation of MODIS aerosol retrieval over ocean *Geophys. Res. Lett.* **29** 1618

Saha A and Despiau S 2009 Seasonal and diurnal variations of black carbon aerosols over a Mediterranean coastal zone *Atmos. Res.* **92** 27–41

Sahu LK and Sheel V 2014 Spatio-temporal variation of biomass burning sources over South and Southeast Asia *J. Atmos. Chem.* **71** 1–19

Schuster GL, Dubovick O and Holben BN 2006 Angstrom exponent and bimodal aerosol size distributions *J. Geophys. Res.* **111** D07207

Seiler W and Crutzen P J 1980 Estimates of gross and net fluxes of carbon between the biosphere and the atmosphere from biomass burning *Clim. Change* **2** 207–47

Tanré D *et al* 1997 Remote sensing of aerosol properties over oceans using the MODIS/EOS spectral radiances *J. Geophys. Res.* **102** 16971–88

Taylor D 2010 Biomass burning, humans and climate change in Southeast Asia *Biodiversity Conservation* **19** 1025–42

Toky OP and Ramakrishnan PS 1983 Secondary succession following slash and burn agriculture in North-Eastern India: I. biomass, litterfall and productivity *J. Ecology* **71** 735–45

Torres O et al 1998 Derivation of aerosol properties from satellite measurements of backscattered ultraviolet radiation: theoretical basis J. Geophys. Res. Atmos. 103 17099e17110
Torres O et al 2007 Aerosols and surface UV products from ozone monitoring instrument observations: an overview J. Geophys. Res. 112 D24S47
Torres O et al 2010 OMI and MODIS observations of the anomalous 2008–2009 Southern Hemisphere biomass burning seasons Atmos. Chem. Phys. 10 3505–13
Torres O et al 2012 Retrieval of aerosol optical depth above clouds from OMI observations: sensitivity analysis and case studies J. Atmos. Sci. 69 1037–53
Vadrevu K P et al 2011 MODIS derived fire characteristics and aerosol optical depth variations during the agricultural residue burning season, north India Environ. Pollut. 159 1560–9
Vadrevu K P et al 2013 Hotspot analysis of vegetation fires and intensity in the Indian region IEEE J. Sel. Top. Appl. Earth Obs. Remote Sens. 6 224–38
Vaughan MA et al 2004 Fully automated analysis of space-based lidar data: an overview of the CALIPSO retrieval algorithms and data products Proc. SPIE 5575 16–30
Winker D M 2007 Initial performance assessment of CALIOP Geophys. Res. Lett. 34 19803
Xia X, Zong X and Sun L 2013 Exceptionally active agricultural fire season in mid-eastern China in June 2012 and its impact on the atmospheric environment J. Geophys. Res. 118 9889–900